

MEASURE TWICE, CUT ONCE: A SEMANTIC-ORIENTED APPROACH TO VIDEO TEMPORAL LOCALIZATION WITH VIDEO LLMs

Zongshang Pang¹ Mayu Otani² Yuta Nakashima¹

¹The University of Osaka ²CyberAgent, Inc.

{pangzs, n-yuta}@im.sanken.osaka-u.ac.jp otani_mayu@cyberagent.co.jp

ABSTRACT

Temporally localizing user-queried events through natural language is a crucial capability for video models. Recent methods predominantly adapt video LLMs to generate event boundary timestamps for temporal localization tasks, which struggle to leverage LLMs’ pre-trained semantic understanding capabilities due to the uninformative nature of timestamp outputs. In this work, we explore a timestamp-free, semantic-oriented framework that fine-tunes video LLMs using two generative learning tasks and one discriminative learning task. We first introduce a structural token generation task that enables the video LLM to recognize the temporal structure of input videos based on the input query. Through this task, the video LLM generates a sequence of special tokens, called structural tokens, which partition the video into consecutive segments and categorize them as either target events or background transitions. To enhance precise recognition of event segments, we further propose a query-focused captioning task that enables the video LLM to extract fine-grained event semantics that can be effectively utilized by the structural tokens. Finally, we introduce a structural token grounding module driven by contrastive learning to associate each structural token with its corresponding video segment, achieving holistic temporal segmentation of the input video and readily yielding the target event segments for localization. Extensive experiments across diverse temporal localization tasks demonstrate that our proposed framework, MeCo, consistently outperforms methods relying on boundary timestamp generation, highlighting the potential of a semantic-driven approach for temporal localization with video LLMs¹.

1 INTRODUCTION

Localizing temporal events based on user interests is an essential capability for video recognition systems to handle practical video tasks such as moment retrieval (Lei et al., 2021), action localization (Chao et al., 2018; Cheng & Bertasius, 2022), video summarization (Song et al., 2015; Gygli et al., 2014), and dense video captioning (Krishna et al., 2017; Wang et al., 2021a; Yang et al., 2023). While such temporal localization tasks were traditionally handled by specialist models, recent research has begun leveraging video LLMs to unify them within a single framework by adapting LLMs for boundary timestamp generation (Ren et al., 2024; Liu et al., 2024c; Zeng et al., 2025).

Accurately localizing the boundary timestamps of a target event requires understanding the semantic content of the target event by both examining its relevance to the localization query (*e.g.*, an event description or action label) and differentiating it from adjacent events to identify event boundaries. However, current methods expect video LLMs to internally handle the semantic understanding and directly provide the final boundary timestamps. Consequently, a major focus of this line of research has been to develop various video LLM-friendly timestamp representations to boost performance. Nonetheless, direct timestamp generation may limit the potential of video LLMs, as they are backed by LLMs that are built to process semantic information (Brown et al., 2020) and have primarily been pre-trained on video captioning and question answering tasks that require mapping visual inputs to

¹Code available at <https://github.com/pangzss/MeCo>.

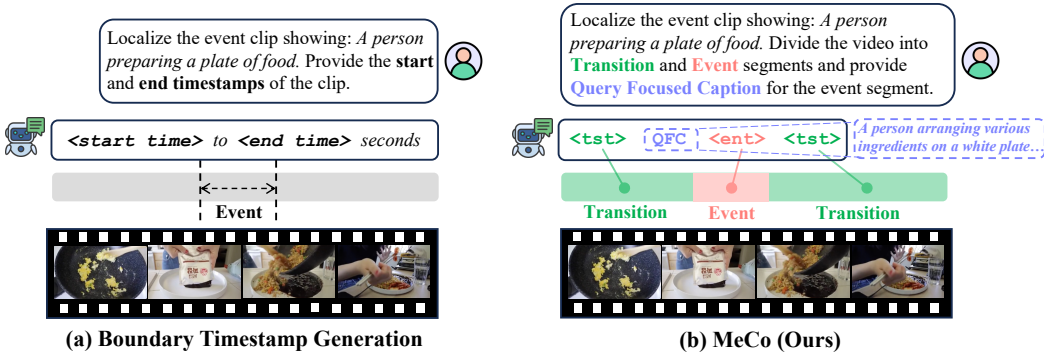


Figure 1: In contrast to previous boundary timestamp generation approaches (Ren et al., 2024; Guo et al., 2025a; Liu et al., 2024c; Huang et al., 2024; 2025; Guo et al., 2025b), MeCo leverages the semantic understanding capability of video LLMs to capture the video temporal structure and categorize video segments into transition and event structural tokens `<tst>` and `<ent>`. It can also generate query-focused captions (QFC) to scrutinize the detailed event semantics, which can facilitate more accurate localization of the event segment via the event token. The semantic-oriented pipeline completely frees video LLMs from timestamps generation.

outputs with concrete semantic meanings (Maaz et al., 2023; Lin et al., 2023a). Additionally, it has been shown that LLMs struggle with highly uninformative outputs in both language (Wei et al., 2022; Kojima et al., 2022) and multimodal scenarios (Lai et al., 2024; Liu et al., 2024c). In this work, we initiate the exploration of semantic-oriented strategies for adapting video LLMs to video temporal localization tasks. We adapt video LLMs’ semantic understanding ability for such tasks through carefully designed supervised fine-tuning tasks involving both generative and discriminative learning objectives.

To start, we propose a *structural token generation* task to enable the video LLM to distinguish semantic differences between queried events and background transitions by capturing the overall temporal video structure. The output consists of consecutive segments in the video categorized as a sequence of *event tokens* `<ent>` and *transition tokens* `<tst>`, arranged in temporal order. To facilitate more precise categorization of event segments via event structural tokens, we propose a *query-focused captioning* task that enables the video LLM to scrutinize the details in each queried event before localization by generating detailed captions for it, akin to the role of Chain-of-Thoughts before LLMs’ final answers (Wei et al., 2022; Kojima et al., 2022). These two tasks exploit the innate generative power of video LLMs to adapt their semantic understanding abilities for temporal localization tasks.

Building on the temporal categorization from structural tokens and the semantic refinement from query-focused captions, we propose a *structural token grounding* module based on contrastive learning (He et al., 2020; Radford et al., 2021; Wang et al., 2021b; Oquab et al., 2023; Pang et al., 2024) to map the rich semantics encoded in each structural token to the corresponding video segments. This enables holistic video segmentation, where queried events can be precisely localized through their corresponding structural tokens. The contrastive learning objective effectively taps into the hidden discriminative power of LLMs (BehnamGhader et al., 2024; Liu et al., 2024c) for temporal localization tasks.

The proposed framework, named MeCo, enables video LLMs to **M**easure twice by prioritizing the semantic understanding of holistic video structure and fine-grained event content before **C**utting **o**nce to extract all queried event segments. This design fundamentally differs from timestamp generation-centric approaches, making MeCo a fully semantic-centric approach for video LLM-based temporal localization. An illustration of the three proposed objectives is shown in Fig. 1. Extensive experiments show that MeCo consistently outperforms timestamp-centric approaches, often by significant margins, across 9 tasks spanning grounding, dense video captioning, and complex reasoning domains (Liu et al., 2024c).

2 RELATED WORK

Video Temporal Localization Tasks. Video temporal localization tasks such as moment retrieval and highlight detection (Lei et al., 2021), extractive video summarization (Gygli et al., 2014; Song et al., 2015; Pang et al., 2023), and action localization (Chao et al., 2018; Cheng & Bertasius, 2022) require localizing salient event segments in response to a user query in the form of event boundary timestamps. Furthermore, tasks such as dense video captioning (Krishna et al., 2017; Yang et al., 2023) and grounded video question answering (Bärmann & Waibel, 2022; Di & Xie, 2024) involve generating captions and performing complex reasoning about these localized events. Traditionally, these tasks have been addressed by specialist models with task-specific designs and domain-specific training data. Although unified models for localization-only tasks have been proposed (Lin et al., 2023c; Yan et al., 2023; Liu et al., 2024b), they cannot handle generative tasks like captioning.

Video LLMs. Early efforts to enable LLMs to perform video-level tasks used LLMs as agents built on chain-of-thought reasoning and tool-use mechanisms (Zeng et al., 2022; Surís et al., 2023; Lin et al., 2023b). Advances in end-to-end multimodal pretraining (Radford et al., 2021; Li et al., 2023) and instruction tuning (Ouyang et al., 2022; Liu et al., 2024a) have led to the development of powerful video LLMs (Zhang et al., 2023; Song et al., 2024; Li et al., 2024; Wang et al., 2024b; Li et al., 2025; Yuan et al., 2025), which have shown that these models excel at temporal reasoning over very long videos, benefiting from LLMs’ long-context semantic retrieval abilities. However, while effective for general video understanding tasks such as captioning and question answering, they do not address tasks that require event temporal localization.

Temporal Localization Video LLMs. Recent developments in temporal localization video LLMs have enabled unified approaches for both localization and generation tasks. Models such as TimeChat (Ren et al., 2024) fine-tune pre-trained video LLMs to output numeric tokens that represent event boundary timestamps. Subsequent works (Huang et al., 2025; Qian et al., 2024; Guo et al., 2025a;b) augment the LLM’s vocabulary with learnable timestamp tokens. For example, VTG-LLM represents timestamps with a set of learnable digit tokens and pads the timestamp token sequence to a fixed length (Guo et al., 2025a). Meanwhile, TRACE introduces specialized timestamp encoder and decoder (Guo et al., 2025b) and VideoChat-T proposes a temporal adaptive position encoding module (Zeng et al., 2025). There are also works that directly interleave the textual timestamps with frame tokens (Meinardus et al., 2024; Lu et al., 2024). Observing that LLMs struggle with numeric tokens and many newly introduced tokens, E.T. Chat (Liu et al., 2024c) instead fine-tunes LLMs on a boundary embedding matching task using a single boundary matching token. As a departure from such works relying on timestamp generation, we propose MeCo to explore how the innate semantic understanding capabilities of video LLMs can be leveraged to build a unified temporal localization framework.

3 METHOD

3.1 OVERVIEW

Video temporal localization involves understanding user-queried events and determining their temporal boundaries $\{(t_i^s, t_i^e)\}_{i=1}^M$ with $M \geq 1$. Depending on the query, the localized boundaries should sometimes be accompanied by event captions (Krishna et al., 2017) or answers to event-related questions (Bärmann & Waibel, 2022), which are treated as textual tokens $\{x_n\}_{n=1}^N$, where N is the total number of tokens. Recently, such temporal localization tasks have been unified within a single video LLM-based framework (Ren et al., 2024; Guo et al., 2025a).

Current video LLM-based methods focus on boundary timestamp generation, which fails to leverage video LLMs’ core strength: their pre-trained semantic understanding capabilities. In contrast, we leverage video LLMs’ semantic understanding and retrieval capabilities to partition the input video into segments, categorize them as target events or background transitions, and summarize their semantics in the hidden states of the proposed structural tokens. To ensure precise retrieval of event semantics, we augment the structural tokens with query-focused captions. Finally, the structural token grounding module maps the structural tokens to their corresponding video segments via the retrieved and summarized semantics in their hidden states. We now describe in detail how we equip the video LLM with these capabilities. An illustration of the proposed components is in Fig. 2.

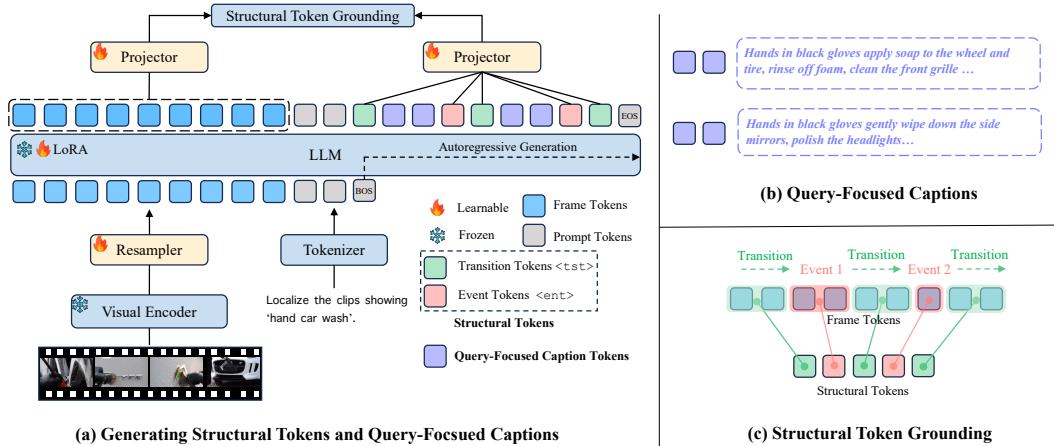


Figure 2: Overview of the proposed MeCo framework. Given an input video and a localization-related user query, MeCo generates **structural tokens** (Sec. 3.2), including the event token $\langle \text{ent} \rangle$ and the transition token $\langle \text{tst} \rangle$, enhanced by **query-focused captions** (Sec. 3.3) to encode more precise semantic information and can facilitate holistic temporal segmentation via **structural token grounding** (Sec. 3.4).

3.2 STRUCTURAL TOKEN GENERATION

Although video LLMs have demonstrated excellent temporal structure understanding for video question answering through causal reasoning and for video captioning by describing narrative flow (Song et al., 2024; Wang et al., 2024c; Zhang et al., 2024; Xue et al., 2024), this capability has not yet been explicitly leveraged for temporal localization. To fill this gap, we propose a novel structural token generation task for training the video LLM to materialize its temporal structure understanding into a temporally ordered sequence of video segments to facilitate temporal localization.

Given a T -frame video as input², a visual encoder (Fang et al., 2023b) and a resampler (Liu et al., 2024c) from the video LLM extract from the video a set of frame feature maps $\{\mathbf{F}_t\}_{t=1}^T$, where $\mathbf{F}_t \in \mathbb{R}^{P \times C}$ has P token embedding vectors, each of dimension C . An LLM decoder then takes $\{\mathbf{F}_t\}_{t=1}^T$ and the tokenized user query $\{q_l\}_{l=1}^L$ as inputs. The structural token generation task requires the video LLM to distinguish between event segments and background transition segments in the input video based on the user query. The segments are then represented in the LLM’s autoregressively generated output as either *event tokens* $\langle \text{ent} \rangle$ or *transition tokens* $\langle \text{tst} \rangle$, collectively called *structural tokens*, which are newly added to the LLM vocabulary before fine-tuning.

The preparation of supervised fine-tuning data for the structural token generation task builds on ground-truth event boundary timestamps from general temporal localization data. Given a T -frame video with a set of M ground-truth event boundary timestamps $\{(t_i^s, t_i^e)\}_{i=1}^M$, we augment them with neighboring transition segments to form an augmented set of segments $\{(t_i^s, t_i^e)\}_{i=1}^{M+K}$, where K is the total number of transition segments. Let \mathbb{I}_{ent} be the set of indices of

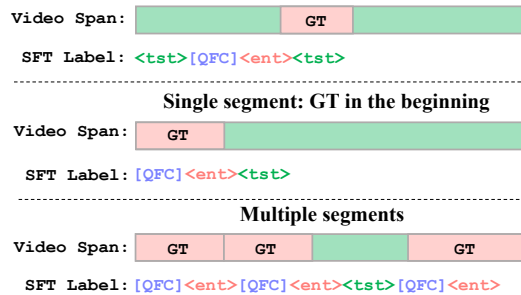


Figure 3: Examples of supervised fine-tuning (SFT) labels created from temporal localization data, where GT stands for Ground Truth windows and QFC for Query-Focused Caption (Sec. 3.3). For illustration clarify, we only show non-overlapping events for the multi-segment scenario, as overlapping events can be represented in a way similar to consecutive events, e.g., $[\text{QFC}] \langle \text{ent} \rangle [\text{QFC}] \langle \text{ent} \rangle$.

²By default, we sample frames from videos at 1 fps unless specified otherwise.

the queried event segments; the sequence of structural tokens can be defined as $\{\text{ST}(i)\}_{i=1}^{M+K}$ with

$$\text{ST}(i) = \begin{cases} \langle \text{ent} \rangle & \text{if } i \in \mathbb{I}_{\text{ent}}, \\ \langle \text{tst} \rangle & \text{otherwise.} \end{cases} \quad (1)$$

Importantly, event segments may appear at video boundaries or occur consecutively without intervening transitions. These cases provide crucial learning signals: the $\langle \text{tst} \rangle$ token does not always trivially precede and follow the $\langle \text{ent} \rangle$ token, and should only appear based on the actual presence of transition segments in the video. Several illustrative examples are provided in Fig. 3. Overall, structural tokens transform the video’s temporal flow into a sequence of events and transitions. Through auto-regressive generation, each structural token must attend to its corresponding segment, thereby summarizing the segment’s semantic information in its hidden state. This creates the foundation for grounding structural tokens to their corresponding video segments for localization purposes.

3.3 QUERY-FOCUSED CAPTIONING

Just as humans rewatch clips to identify specific details of interest, we hypothesize that the summarized segment semantics encoded in structural tokens can be refined by having the LLM examine each event segment more closely. To this end, we introduce a query-focused captioning task that requires the model to generate detailed captions for queried segments. By generating these captions immediately before each corresponding event token $\langle \text{ent} \rangle$, we provide rich semantic information that the token can attend to via causal attention. This process mirrors chain-of-thought reasoning (Wei et al., 2022), where intermediate reasoning steps enhance the quality of final outputs, but resorts to more obtainable captions.

As shown in Fig. 2 and Fig. 3, the overall tokens that the LLM needs to generate now become an interleaved sequence of structural tokens and query-focused caption tokens $\mathbf{X} = \{\text{CAP}(i), \text{ST}(i)\}_{i=1}^{M+K}$ with

$$\text{CAP}(i) = \begin{cases} [\text{QFC}]_i & \text{if } i \in \mathbb{I}_{\text{ent}}, \\ \emptyset & \text{otherwise,} \end{cases} \quad (2)$$

where $[\text{QFC}]_i$ encloses all query-focused caption tokens for the i -th event segment, and \emptyset indicates no such token is placed (we omit the end-of-sequence token for notational clarity). It is worth noting that textual response tokens for tasks involving captioning and question answering are treated as part of the query-focused caption tokens to unify the output format across all temporal localization tasks. The training objectives of structural token generation and query-focused captioning can be unified as a single language modeling loss:

$$\mathcal{L}_{\text{LM}} = -\frac{1}{N} \sum_{n=1}^N \log p(\mathbf{X}_n | \{\mathbf{F}_t\}_{t=1}^T, \{\mathbf{q}_i\}_{i=1}^L, \mathbf{X}_{<n}), \quad (3)$$

where \mathbf{X}_n is the n -th token in \mathbf{X} , $\mathbf{X}_{<n} = \{\mathbf{X}_{n'}\}_{n'=1}^{n-1}$, and N is the total number of tokens in \mathbf{X} .

As query-focused captioning is a novel task with no existing dataset, we leverage the ground-truth event timestamps in E.T.Instruct (Liu et al., 2024c) to extract event clips, which are then sent to a video captioning model to generate detailed clip captions. Further details regarding the generation pipeline are presented in the Appendix C.

3.4 STRUCTURAL TOKEN GROUNDING

To ground the generated structural tokens to their corresponding video segments, we leverage LLM hidden states to maximize the log-likelihood of the structural tokens with respect to their corresponding segment frames. Formally, given the projected LLM hidden states $\{\mathbf{H}_t\}_{t=1}^T$ and $\{\mathbf{s}_i\}_{i=1}^{M+K}$ (from two learnable MLP projectors following Liu et al. (2024c)) of the video frames and the structural tokens, respectively, where $\mathbf{H}_t \in \mathbb{R}^{P \times C}$ and $\mathbf{s}_i \in \mathbb{R}^C$, the structural token grounding loss can be formulated as:

$$\mathcal{L}_{\text{ST}} = -\frac{1}{M+K} \sum_{i=1}^{M+K} \sum_{t=t_i^s}^{t_i^e} \frac{\log p(\mathbf{h}_t | \mathbf{s}_i)}{t_i^e - t_i^s}, \quad (4)$$

where $\mathbf{h}_t \in \mathbb{R}^C$ is spatially average-pooled from \mathbf{H}_t , τ is a learnable temperature parameter (Radford et al., 2021), and both \mathbf{h}_t and \mathbf{s}_i are normalized to the unit sphere following (Radford et al., 2021; He et al., 2020). The conditional probability $p(\mathbf{h}_t|\mathbf{s}_i)$ of frame t given structural token i is computed as:

$$p(\mathbf{h}_t|\mathbf{s}_i) = \frac{\exp(\mathbf{s}_i \cdot \mathbf{h}_t / \tau)}{\sum_{t'=1}^T \exp(\mathbf{s}_i \cdot \mathbf{h}_{t'} / \tau)}, \quad (5)$$

which essentially makes Eq. (4) a contrastive learning objective (He et al., 2020; Radford et al., 2021) that pulls together structural tokens and their corresponding segment frames. We also attempted the symmetric version of Eq. (4) by including $p(\mathbf{s}_i|\mathbf{h}_t)$, similar to Radford et al. (2021), but observed performance drops, for which we provide analysis in Sec. 4.4, and thus we choose Eq. (4) as the final loss function.

3.5 TRAINING AND INFERENCE

The overall training objective of the video LLM is a combination of the language modeling loss and the structural token grounding loss:

$$\mathcal{L} = \mathcal{L}_{\text{LM}} + \mathcal{L}_{\text{ST}}, \quad (6)$$

where \mathcal{L}_{LM} and \mathcal{L}_{ST} are defined in Eq. (3) and Eq. (4), respectively. We use the E.T. Instruct dataset (Liu et al., 2024c) containing 164K samples augmented with query-focused captions and updated instructions as the supervised fine-tuning dataset. More details regarding the dataset and instructions are provided in Appendix C and Appendix G.

During inference, the video LLM recognizes the video’s temporal structure to determine the presence of event and transition segments, and then auto-regressively generates corresponding structural tokens (<ent> and <tst>). Before generating each <ent> token, the model first produces a query-focused caption for that event segment. Upon completion of structural token generation indicated by the end-of-sentence token <EOS>, we compute $p(\mathbf{h}_t|\mathbf{s}_i)$ as in Eq. (5) for all frames with respect to each structural token. We then obtain holistic temporal segmentation by assigning each frame to the structural token that yields the highest conditional probability. This directly yields the queried event segments via the event tokens <ent>. The pseudocode for MeCo inference is provided in Appendix E.

4 EXPERIMENTS

4.1 BENCHMARKS

We evaluate MeCo’s zero-shot temporal localization performance on three benchmarks: E.T. Bench (Liu et al., 2024c), Charades-STA (Gao et al., 2017), and QVHighlights (Lei et al., 2021).

E.T. Bench is a comprehensive benchmark composed of curated data from various public benchmarks for event-level and time-sensitive video tasks. We utilize the grounding, dense captioning, and complex temporal reasoning domains in E.T. Bench for evaluating our method. The grounding domain, with F1 score as the evaluation metric, includes five tasks: Temporal Video Grounding (TVG) (Lei et al., 2021; Gao et al., 2017), Episodic Memory (EPM) (Grauman et al., 2022), Temporal Action Localization (TAL) (Patraucean et al., 2023; Gorban et al., 2015; Jiang et al., 2014), Extractive Video Summarization (EVS) (Song et al., 2015; Gygli et al., 2014), and Video Highlight Detection (VHD) (Song et al., 2015; Gygli et al., 2014). The dense captioning domain, with F1 score and sentence similarity as the evaluation metrics, consists of two tasks: Dense Video Captioning (DVC) (Zala et al., 2023; Zhou et al., 2018) and Step Localization and Captioning (SLC) (Zhukov et al., 2019; Afouras et al., 2023). The complex temporal reasoning domain, with recall as the evaluation metric, includes two tasks: Temporal Event Matching (TEM) (Patraucean et al., 2023; Lei et al., 2021) and Grounded Video Question Answering (GVQ) (Bärmann & Waibel, 2022).

Charades-STA and QVHighlights are widely adopted benchmarks for temporal grounding and video highlight detection. The TVG task of E.T. Bench contains samples from both these two benchmarks, but does not evaluate the highlight detection performance for QVHighlights. We thus report additional results directly on the original benchmarks to facilitate comparisons with existing methods. For Charades-STA (Gao et al., 2017), we use recall at temporal Intersection over Union thresh-

Table 1: Zero-shot performance comparisons on E.T. Bench. ‘‘SFT. Data’’ refers to the supervised fine-tuning data used in the temporal localization tuning stage, which may include both localization-specific and other video data. **Grayed out** metrics are not zero-shot results as the model accessed the training data of the corresponding evaluation data in E.T. Bench. **Bold** and *italic* only are used for comparisons in the self-implemented E.T.Instruct fine-tuning-based setting.

| Model | SFT Data | Epochs | LoRA | Grounding | | | | | Dense Captioning | | | | Complex | |
|--|----------|--------|------|-------------------|-------------------|-------------------|-------------------|-------------------|-------------------|--------------------|-------------------|--------------------|--------------------|--------------------|
| | | | | TVG _{F1} | EPM _{F1} | TAL _{F1} | EVS _{F1} | VHD _{F1} | DVC _{F1} | DVC _{Sim} | SLC _{F1} | SLC _{Sim} | TEM _{Rec} | GVQ _{Rec} |
| <i>Video LLMs prompted with timestamps by Liu et al. (2024c)</i> | | | | | | | | | | | | | | |
| Video-ChatGPT (7B) (Maaz et al., 2023) | - | - | - | 7.0 | 1.3 | 15.1 | 8.4 | 28.8 | 8.8 | 11.3 | 5.7 | 10.2 | 15.9 | 0.0 |
| PLLaVA (7B) (Xu et al., 2024) | - | - | - | 6.9 | 1.1 | 5.7 | 0.3 | 28.9 | 13.3 | 10.6 | 9.7 | 11.8 | 4.1 | 1.2 |
| Video-LLaVA (7B) (Lin et al., 2023a) | - | - | - | 7.0 | 1.9 | 15.0 | 0.3 | 28.9 | 28.0 | 15.0 | 0.9 | 8.3 | 7.5 | 0.1 |
| Video-LLaMA-2 (7B) (Zhang et al., 2023) | - | - | - | 0.1 | 0.0 | 0.0 | 0.0 | 1.5 | 0.6 | 14.5 | 0.0 | 15.2 | 0.0 | 0.1 |
| <i>Temporal Localization video LLMs trained with their respective settings.</i> | | | | | | | | | | | | | | |
| VTimeLLM (7B) (Huang et al., 2024) | 142K | 2 | ✓ | 7.6 | 1.9 | 18.2 | 15.9 | 28.9 | 12.4 | 13.1 | 8.7 | 6.4 | 6.8 | 1.9 |
| VTG-LLM (7B) (Guo et al., 2025a) | 217K | 10 | ✓ | 15.9 | 3.7 | 14.4 | 26.8 | 48.2 | 40.2 | 18.6 | 20.8 | 14.4 | 8.9 | 1.4 |
| TimeChat (7B) (Ren et al., 2024) | 198K | 3 | ✓ | 26.2 | 3.9 | 10.1 | 29.1 | 40.5 | 16.6 | 12.5 | 5.6 | 9.2 | 18.0 | 1.5 |
| LITA (13B) (Huang et al., 2025) | 500K | 1 | × | 22.2 | 4.6 | 18.0 | 29.7 | 23.9 | 39.7 | 17.2 | 21.0 | 12.2 | 16.0 | 2.2 |
| TRACE (7B) (Guo et al., 2025a) | 900K | 2 | × | 44.3 | 11.1 | 19.1 | 27.4 | 65.9 | 46.4 | 23.7 | 28.3 | 18.1 | 19.2 | 0.0 |
| Dispider (7B) (Qian et al., 2025) | 639K | 1 | × | 43.6 | 17.2 | 29.9 | - | 51.5 | 31.6 | 17.8 | 14.1 | 11.7 | - | - |
| E.T.Chat (3.8B) (Liu et al., 2024c) | 164K | 1 | ✓ | 38.6 | 10.2 | 30.8 | 25.4 | 62.5 | 38.4 | 19.7 | 24.4 | 14.6 | 16.5 | 3.7 |
| <i>Fine-tuned on E.T.Instruct by Yuan et al. (2025)</i> | | | | | | | | | | | | | | |
| Tarsier (7B) (Wang et al., 2024a) | - | - | - | 39.6 | 9.0 | 25.0 | 25.4 | 47.6 | 42.8 | 19.1 | 23.7 | 15.2 | - | - |
| Tarsier2 (7B) (Yuan et al., 2025) | - | - | - | 38.4 | 11.0 | 31.8 | 19.4 | 66.8 | 46.5 | 28.8 | 24.6 | 16.4 | - | - |
| QWen2-VL (7B) (Wang et al., 2024b) | - | - | - | 39.7 | 7.0 | 26.9 | 17.1 | 66.9 | 44.3 | 25.3 | 25.7 | 15.6 | - | - |
| <i>Initialized from the last pre-trained checkpoint without seeing localization data and fine-tuned on E.T.Instruct. Self-implemented.</i> | | | | | | | | | | | | | | |
| VTG-LLM (7B) (Guo et al., 2025a) | - | - | - | 20.0 | 1.5 | 17.6 | 19.5 | 41.6 | 39.9 | 19.6 | 19.6 | 13.6 | 18.2 | 0.3 |
| TimeChat (7B) (Ren et al., 2024) | - | - | - | 24.3 | 2.3 | 17.7 | 23.6 | 43.0 | 39.4 | 16.5 | 18.0 | 11.8 | 19.1 | 0.8 |
| TRACE (7B) (Guo et al., 2025a) | - | - | - | 18.5 | 2.2 | 22.3 | 26.7 | 38.2 | 39.0 | 17.5 | 23.4 | 13.7 | 12.5 | 1.4 |
| E.T.Chat (3.8B) (Liu et al., 2024c) | 164K | 1 | ✓ | 38.6 | 10.2 | 30.8 | 25.4 | 62.5 | 38.4 | 19.7 | 24.4 | 14.6 | 16.5 | 3.7 |
| MeCo (ETChat 3.8B) | - | - | - | 59.1 | 11.2 | 32.6 | 33.2 | 66.9 | 43.4 | 20.3 | 27.3 | 15.7 | 23.6 | 9.6 |
| MeCo (ETChat 7B) | - | - | - | 62.5 | 15.4 | 35.1 | 35.1 | 66.3 | 43.4 | 20.7 | 30.1 | 16.5 | 19.1 | 9.9 |
| MeCo (QWen2VL 7B) | - | - | - | 59.0 | 17.5 | 34.2 | 35.5 | 67.9 | 41.5 | 22.8 | 28.1 | 16.5 | 15.4 | 15.1 |

olds of 0.3 (R@1_{0.3}), 0.5 (R@1_{0.5}) and 0.7 (R@1_{0.7}). For QVHighlights, we use mean Average Precision (mAP) and HIT@1 for highlight detection.

4.2 IMPLEMENTATION DETAILS

We develop MeCo using the E.T.Chat (Liu et al., 2024c) QWen2VL-7B (Wang et al., 2024b). For ETChat, we use its original Phi-3-Mini-3.8B (Abdin et al., 2024) version and implement a 7B version based on QWen2-7B (Yao et al., 2024) by following ETChat’s three-stage training protocol, where the final stage involves temporal localization fine-tuning with LoRA (Hu et al., 2021) for one epoch. For QWen2VL-7B, we directly fine-tune the pre-trained checkpoint plus the newly initialized projectors from ETChat with the temporal localization data. More implementation details are provided in Appendix B.

4.3 MAIN RESULTS

E.T. Bench: Comprehensive comparisons. As shown in Tab. 1, although previous temporal localization video LLMs demonstrate promising zero-shot results compared to general video LLMs, they underperform on most tasks compared to MeCo. Specifically, MeCo (3.8B) achieves substantial gains across all domains. Notably, many models use larger base LLMs and train for considerably more steps. The results demonstrate that MeCo leverages video LLMs’ semantic understanding more effectively for temporal localization than boundary-centric methods. Furthermore, when MeCo uses a more powerful base LLM (7B), its performance consistently improves on most tasks, reinforcing its scalability and effectiveness.

E.T. Bench: Comparisons with E.T.Instruct fine-tuning. When fine-tuned on E.T.Instruct, VTG-LLM (Guo et al., 2025a) and TimeChat (Ren et al., 2024) retain performance levels comparable to their original settings. TRACE (Guo et al., 2025b) experiences the greatest performance drop, likely because its specialized timestamp encoder/decoder and newly introduced timestamp tokens require extensive tuning for effective adaptation to the LLM. In contrast, MeCo emphasizes leveraging the inherent semantic understanding of video LLMs, making it more amenable to efficient fine-tuning.

Temporal Grounding. As shown in Tab. 2, MeCo achieves consistently better zero-shot performance on Charades-STA compared to either previous methods’ official checkpoints or E.T.Instruct-fine-tuned checkpoints. After fine-tuning on the training set of Charades-STA, MeCo achieves significantly better results and retain the best performance for R@1_{0.3} and R@1_{0.5}. However, MeCo prioritizes capturing general semantic differences between query-relevant and background frames

Table 2: Zero-shot and dataset-wise fine-tuning performance on Charades-STA and QVHighlights.

| Model | Charades-STA | | | QVHighlights | |
|--|--------------------|--------------------|--------------------|--------------|-------|
| | R@1 _{0.3} | R@1 _{0.5} | R@1 _{0.7} | mAP | HIT@1 |
| <i>Zero-shot performance (official checkpoints).</i> | | | | | |
| VTimeLLM (7B) (Huang et al., 2024) | 51.0 | 27.5 | 11.4 | - | - |
| VTimeLLM (13B) (Huang et al., 2024) | 55.3 | 34.3 | 14.7 | - | - |
| Momentor (7B) (Qian et al., 2024) | 42.6 | 26.6 | 11.6 | 7.6 | - |
| HawkEye (7B) (Wang et al., 2024d) | 50.6 | 31.4 | 4.5 | - | - |
| TimeChat (7B) (Ren et al., 2024) | - | 32.2 | 13.4 | 14.5 | 23.9 |
| VTG-LLM (7B) (Guo et al., 2025a) | - | 33.8 | 15.7 | 16.5 | 33.5 |
| TRACE (7B) (Guo et al., 2025b) | - | 40.3 | 19.4 | 26.8 | 42.7 |
| E.T.Chat (3.8B) (Liu et al., 2024c) | 64.4 | 43.2 | 19.4 | 23.2 | 58.9 |
| Seq2Time (7B) (Deng et al., 2025) | - | 31.2 | 13.7 | - | - |
| NumPro-FT (7B) (Wu et al., 2025) | 63.8 | 42.0 | 20.6 | 25.0 | 37.2 |
| VideoChat-T (7B) (Zeng et al., 2025) | 69.9 | 48.7 | 24.0 | 26.5 | 54.1 |
| <i>Zero-shot performance (Fine-tuned on E.T.Instruct).</i> | | | | | |
| TimeChat (7B) (Ren et al., 2024) | 43.4 | 24.9 | 9.2 | 16.4 | 30.6 |
| VTGLLM (7B) (Guo et al., 2025a) | 24.8 | 9.8 | 3.5 | 15.9 | 27.1 |
| TRACE (7B) (Guo et al., 2025b) | 39.4 | 23.7 | 11.5 | 16.4 | 30.6 |
| E.T.Chat (3.8B) (Liu et al., 2024c) | 64.4 | 43.2 | 19.4 | 23.2 | 58.9 |
| MeCo (ETChat 3.8B) | 66.7 | 44.4 | 17.5 | 39.2 | 61.8 |
| MeCo (ETChat 7B) | 69.6 | 46.4 | 19.1 | 39.5 | 64.3 |
| MeCo (QWen2VL 7B) | 71.1 | 50.1 | 23.3 | 37.2 | 57.9 |
| <i>Dataset-wise fine-tuning performance.</i> | | | | | |
| M-DETR (Lei et al., 2021) | 65.8 | 52.1 | 30.6 | 35.7 | 55.6 |
| UMT (Liu et al., 2022) | - | - | - | 39.9 | 64.2 |
| QD-DETR (Moon et al., 2023b) | - | 57.3 | 32.6 | 39.1 | 63.0 |
| CG-DETR (Moon et al., 2023a) | 70.4 | 58.4 | 36.3 | 40.8 | 66.7 |
| UniVTG (Lin et al., 2023c) | 72.6 | 60.2 | 38.6 | 38.8 | 61.8 |
| HawkEye (7B) (Wang et al., 2024d) | 72.5 | 58.3 | 28.8 | - | - |
| TimeChat (7B) (Ren et al., 2024) | - | 46.7 | 23.7 | 21.7 | 37.9 |
| VTG-LLM (7B) (Guo et al., 2025a) | - | 57.2 | 33.4 | - | - |
| TRACE (7B) (Guo et al., 2025b) | - | 61.7 | 41.4 | - | - |
| VideoChat-T (7B) (Zeng et al., 2025) | 79.4 | 67.1 | 43.0 | 27.0 | 55.3 |
| MeCo (ETChat 3.8B) | 75.3 | 61.6 | 38.5 | 44.6 | 71.8 |
| MeCo (ETChat 7B) | 77.2 | 63.9 | 40.1 | 44.7 | 74.3 |
| MeCo (QWen2VL 7B) | 82.3 | 68.5 | 41.6 | 45.3 | 75.1 |

rather than modeling dataset-specific phase-in and phase-out boundary patterns, it may achieve less impressive gains in terms of R@1_{0.7}.

Highlight detection. As the continuous semantic similarities derived from Eq. (5) can directly be utilized as highlight scores, MeCo achieves much higher performance in mAP and HIT@1 for highlight detection than previous methods, most of which generate numeric tokens to approximate highlight scores which struggle to capture the underlying semantic information. Impressively, fine-tuning with the training set of QVHighlights significantly improves MeCo’s performance, which even prominently surpasses that of the specialist models. Importantly, MeCo is the only method that achieves a decent balance between temporal grounding and highlight detection.

4.4 ABLATION STUDY

In this section, all experiments are conducted with MeCo (3.8B) unless otherwise specified, and all metrics are reported as the average across all tasks within the corresponding domain in E.T. Bench.

Semantic-based methods excel; video LLMs amplify. In Tab. 3, we compare contrastive vision language models with temporal localization video LLMs. For each contrastive model, we compute the cosine similarities between the localization query feature and the frame features (sampled at 1 fps). We then apply a threshold to these similarity scores and merge contiguous points above the threshold as localized segments. Contrastive models built on semantic similarities perform impressively on grounding tasks without additional training. This provides solid proof for the strength of

Table 3: Comparisons between contrastive vision-language models and video LLMs.

| Model | TVG _{F1} | EPM _{F1} | TAL _{F1} | EVS _{F1} | VHD _{F1} |
|---|-------------------|-------------------|-------------------|-------------------|-------------------|
| <i>Contrastive Vision and Language Models</i> | | | | | |
| CLIP-L-14-224 (Radford et al., 2021) | 35.1 | 10.0 | 19.9 | 30.2 | 62.2 |
| EVA-G-14-224 (Fang et al., 2023a) | 39.7 | 12.7 | 21.7 | 31.4 | 61.8 |
| SIGLIP-L-16-384 (Zhai et al., 2023) | 42.5 | 14.1 | 22.5 | 29.8 | 63.4 |
| <i>Temporal Localization video LLMs</i> | | | | | |
| Previous best | 44.3 | 11.1 | 30.8 | 29.7 | 65.9 |
| MeCo (7B) | 62.5 | 15.4 | 35.1 | 35.1 | 66.3 |

Table 5: The necessity of <fst> token and query-focused captioning (QFC).

| Method | F1 _{gnd} | F1 _{cap} | Sim _{cap} | Rec _{com} |
|-----------------------|-------------------|-------------------|--------------------|--------------------|
| <ent> | 26.7 | 15.0 | 14.2 | 9.4 |
| <ent> + <fst> | 38.1 | 33.8 | 20.5 | 14.5 |
| <ent> + QFC | 40.4 | 32.0 | 19.9 | 14.9 |
| <ent> + Query Copying | 26.6 | 15.2 | 14.3 | 9.5 |
| <ent> + <fst> + QFC | 40.6 | 35.4 | 20.3 | 16.6 |

Table 6: The effect of using different variants of the structural token grounding loss \mathcal{L}_{ST} .

| \mathcal{L}_{ST} Variant | F1 _{gnd} | F1 _{cap} | Sim _{cap} | Rec _{com} |
|---|-------------------|-------------------|--------------------|--------------------|
| $\mathcal{L}_{ST}(p(\mathbf{h}_t \mathbf{s}_i))$ | 40.6 | 35.4 | 20.3 | 16.6 |
| $\mathcal{L}_{ST}(p(\mathbf{h}_t \mathbf{s}_i)) + \mathcal{L}_{ST}(p(\mathbf{s}_i \mathbf{h}_t))$ | 39.9 | 33.4 | 15.9 | 15.2 |
| $\mathcal{L}_{ST}(p(\mathbf{h}_i^{seg} \mathbf{s}_i))$ | 23.2 | 23.5 | 12.9 | 13.4 |
| $\mathcal{L}_{ST}(p(\mathbf{h}_i^{seg} \mathbf{s}_i)) + \mathcal{L}_{ST}(p(\mathbf{s}_i \mathbf{h}_i^{seg}))$ | 24.3 | 25.9 | 13.6 | 13.4 |

semantic-based approaches in temporal localization. By harnessing video LLMs’ powerful semantic understanding capabilities, MeCo further amplifies this strength.

Replacing boundary-centric methods with MeCo yields consistent benefits. To isolate the benefits of MeCo, we compare it against boundary-centric methods under their respective settings. As shown in Tab. 4, MeCo consistently outperforms the original methods under the same setting across all tasks. Details of the experiments in Tab. 4 are provided in the Appendix D.

The necessity of both holistic and localized understanding. As shown in Tab. 5, optimizing the structural token grounding loss without transition tokens (<fst>), with segments derived via thresholding, yields significantly poorer performance than when <fst> is used. Notably, <ent> tokens begin to take effect once query-focused captioning (QFC) is introduced. However, replacing QFC with an uninformative query-copying task (Guo et al., 2025b) reduces performance to the level achieved using only <ent> tokens. By combining holistic structural information via <fst> tokens with localized details from QFC, MeCo achieves the best performance.

Sufficient negative samples matter in \mathcal{L}_{ST} . We now discuss the observation that adding a “symmetric” loss term with $p(\mathbf{s}_i|\mathbf{h}_t)$ for \mathcal{L}_{ST} (Eq. (4)) led to performance drops, as mentioned in Sec. 3.4. In $p(\mathbf{h}_t|\mathbf{s}_i)$ (Eq. (5)), \mathbf{h}_t is a *frame*-level feature and \mathbf{s}_i is intended to capture a *segment*. Taking the softmax over frames involves significantly more terms in the summation of Eq. (5) than taking it over the structural tokens, e.g., 100 frames might correspond to only 3 structural tokens. Thus, the losses over $p(\mathbf{h}_t|\mathbf{s}_i)$ and $p(\mathbf{s}_i|\mathbf{h}_t)$ are not “symmetric” in terms of the softmax. Fewer terms in the denominator of Eq. (5) imply fewer negative samples in Eq. (4), which could negatively affect contrastive learning (He et al., 2020), as shown in Tab. 6 (row 2). To highlight the influence of negative samples, we replace the frame-level features in $p(\mathbf{h}_t|\mathbf{s}_i)$ with segment-level features by using $p(\mathbf{h}_i^{seg}|\mathbf{s}_i)$, where $\mathbf{h}_i^{seg} = \frac{1}{t_i^e - t_i^s} \sum_{t=t_i^s}^{t_i^e} \mathbf{h}_t$. This leads to significantly fewer negative samples and drastically reduces performance (row 3-4).

Boundary-centric methods fail to leverage query-focused captioning. As shown in Tab. 7, various methods that focus solely on boundary timestamp generation fail to exploit the rich semantic cues provided by QFC. While the former focuses on phase-in and phase-out changes, the latter em-

Table 4: Comparisons with boundary-centric methods using the same base video LLMs and frame sampling strategies.

| Model | #Frames | F1 _{gnd} | F1 _{cap} | Sim _{cap} | Rec _{com} |
|--------------------------------|---------|-------------------|-------------------|--------------------|--------------------|
| <i>VideoLLaMa (7B)</i> | | | | | |
| + TimeChat (Ren et al., 2024) | | 22.2 | 28.7 | 14.1 | 9.9 |
| + VTGLLM (Guo et al., 2025a) | 96 | 20.0 | 29.7 | 16.6 | 9.3 |
| + MeCo | | 34.3 | 30.2 | 17.0 | 15.7 |
| <i>E.T.Chat Stage-2 (3B)</i> | | | | | |
| + E.T.Chat (Liu et al., 2024c) | 1 fps | 33.5 | 29.1 | 16.3 | 8.6 |
| + MeCo | | 40.6 | 35.4 | 18.0 | 16.6 |

Table 7: Investigation on the compatibility of QFC and different boundary-centric localization strategies, where Positional Embedding is from Ren et al. (2024), Interleaving from Meinardus et al. (2024), and Boundary Matching from Liu et al. (2024c).

| Loc. Strategy | F1 _{gnd} | F1 _{cap} | Sim _{cap} | Rec _{com} |
|--------------------------|-------------------|-------------------|--------------------|--------------------|
| Positional Embedding | 22.8 | 16.2 | 14.0 | 8.7 |
| + QFC | 14.8 | 15.1 | 11.8 | 8.0 |
| Interleaving | 27.1 | 31.8 | 15.9 | 12.4 |
| + QFC | 23.2 | 20 | 14.6 | 6.1 |
| Boundary Matching | 33.5 | 29.1 | 16.3 | 8.6 |
| + QFC | 30.5 | 26.9 | 18.9 | 7.9 |
| Structural Tokens | 38.1 | 33.8 | 20.5 | 14.5 |
| + QFC | 40.6 | 35.4 | 20.3 | 16.6 |

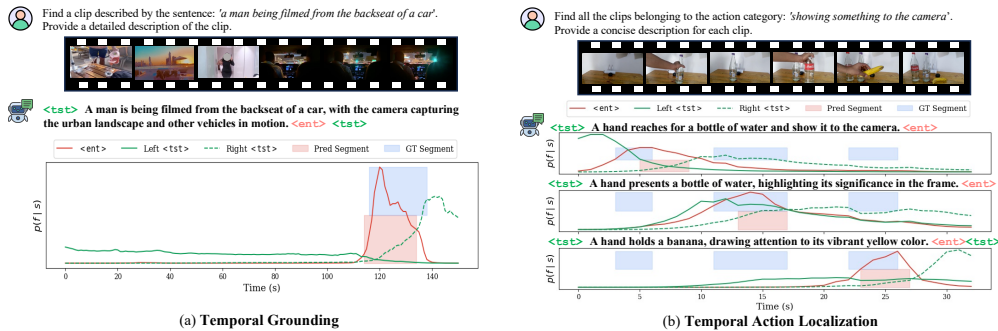


Figure 4: Qualitative examples from temporal grounding and temporal action localization tasks, which involve both single-segment and multi-segment scenarios.

phasizes the most relevant semantic cues. In contrast, MeCo’s structural tokens effectively leverage this detailed semantic information to enhance performance.

Qualitative analysis. As shown in Fig. 4, MeCo can generate detailed query-focused captions and accurately localize event segments in both single-event and multi-event scenarios. However, there remains considerable room for improvement as there still exist predicted windows that are prominently off from the ground-truth. We provide the visualization of failure cases in Appendix Sec. F.

5 CONCLUSION

In this work, we provide a novel perspective of utilizing a semantic-based approach, in contrast to previous boundary-centric methods, to enable video LLMs to handle temporal localization tasks. Instead of directly fine-tuning the video LLMs to generate boundary timestamps, we propose a semantic-oriented framework, MeCo, to better leverage LLM’s pre-trained semantic retrieval capability for temporal localization tasks. MeCo is equipped with structural token generation to capture holistic video structures and query-focused captioning to extract fine-grained event semantics. Facilitated by the structural token grounding module, MeCo can perform a holistic temporal segmentation of the video, readily yielding the timestamps of the queried event segments. Extensive experiments have proven the effectiveness of MeCo on a suite of temporal localization tasks in a zero-shot setting. MeCo also achieves impressive performance in dataset-wise fine-tuning setting for temporal grounding and highlight detection tasks.

6 LIMITATION AND FUTURE WORK

Despite the impressive effectiveness of MeCo, we observed that it has a relatively lower boost in fine-grained grounding metrics, *e.g.*, $R@1_{0.7}$. Intrinsicly, MeCo prioritizes capturing semantic differences between query-relevant and background frames rather than modeling fine-grained phase-in and phase-out boundary patterns. This reflects an inherent trade-off between semantic-oriented strategies that enable strong zero-shot generalization and boundary-focused modeling that excels at fine-grained localization. Thus, we do not claim to totally replace boundary-centric approaches, which inherently enjoy decent compatibility with the generative modeling of LLMs and can directly model the patterns of segment boundaries. Exploring ways to integrate the strengths of both worlds is a promising avenue for future work. Moreover, we believe that the proposed components are by no means the only options for a semantic-oriented approach.

7 ACKNOWLEDGEMENTS

This work was supported by JST ASPIRE Grant No. JPMJAP2502 and JST FOREST Grant No. JPMJFR2160.

8 REPRODUCIBILITY STATEMENT

To enhance the reproducibility of our work, we made the following efforts. Firstly, we provided detailed steps of the training data synthesis process in Sec. 3.2 with visual aid in Fig. 3 and in the appendix Sec. C and Sec. G. Secondly, we provided detailed pseudo code to facilitate the understanding of the inference process in Sec. E. Thirdly, we provided concrete implementation details in the appendix Sec. B and the annotated code base in the supplementary material, which also contains the generated supervised fine-tuning data in the “data/” folder. Finally, we provided all the evaluation instructions in the appendix Sec. G as well the evaluation code in the supplementary material.

REFERENCES

- Marah Abdin, Jyoti Aneja, Hany Awadalla, Ahmed Awadallah, Ammar Ahmad Awan, Nguyen Bach, Amit Bahree, Arash Bakhtiari, Jianmin Bao, Harkirat Behl, et al. Phi-3 technical report: A highly capable language model locally on your phone. *arXiv preprint arXiv:2404.14219*, 2024.
- Triantafyllos Afouras, Effrosyni Mavroudi, Tushar Nagarajan, Huiyu Wang, and Lorenzo Torresani. Ht-step: Aligning instructional articles with how-to videos. *Advances in Neural Information Processing Systems*, 36:50310–50326, 2023.
- Leonard Bärmann and Alex Waibel. Where did i leave my keys?-episodic-memory-based question answering on egocentric videos. In *Proceedings of the IEEE/CVF Conference on Computer Vision and Pattern Recognition*, pp. 1560–1568, 2022.
- Parishad BehnamGhader, Vaibhav Adlakha, Marius Mosbach, Dzmitry Bahdanau, Nicolas Chapados, and Siva Reddy. LLM2Vec: Large Language Models Are Secretly Powerful Text Encoders, 2024.
- Tom Brown, Benjamin Mann, Nick Ryder, Melanie Subbiah, Jared D Kaplan, Prafulla Dhariwal, Arvind Neelakantan, Pranav Shyam, Girish Sastry, Amanda Askell, et al. Language models are few-shot learners. *Advances in neural information processing systems*, 33:1877–1901, 2020.
- Yu-Wei Chao, Sudheendra Vijayanarasimhan, Bryan Seybold, David A Ross, Jia Deng, and Rahul Sukthankar. Rethinking the faster r-cnn architecture for temporal action localization. In *Proceedings of the IEEE conference on computer vision and pattern recognition*, pp. 1130–1139, 2018.
- Feng Cheng and Gedas Bertasius. Tallformer: Temporal action localization with a long-memory transformer. In *European Conference on Computer Vision*, pp. 503–521. Springer, 2022.
- Andong Deng, Zhongpai Gao, Anwesa Choudhuri, Benjamin Planche, Meng Zheng, Bin Wang, Terrence Chen, Chen Chen, and Ziyang Wu. Seq2time: Sequential knowledge transfer for video llm temporal grounding. In *Proceedings of the Computer Vision and Pattern Recognition Conference*, pp. 13766–13775, 2025.
- Shangzhe Di and Weidi Xie. Grounded question-answering in long egocentric videos. In *Proceedings of the IEEE/CVF Conference on Computer Vision and Pattern Recognition*, pp. 12934–12943, 2024.
- Yuxin Fang, Wen Wang, Binhui Xie, Quan Sun, Ledell Wu, Xinggang Wang, Tiejun Huang, Xinlong Wang, and Yue Cao. Eva: Exploring the limits of masked visual representation learning at scale. In *Proceedings of the IEEE/CVF Conference on Computer Vision and Pattern Recognition (CVPR)*, pp. 19358–19369, June 2023a.
- Yuxin Fang, Wen Wang, Binhui Xie, Quan Sun, Ledell Wu, Xinggang Wang, Tiejun Huang, Xinlong Wang, and Yue Cao. Eva: Exploring the limits of masked visual representation learning at scale. In *Proceedings of the IEEE/CVF conference on computer vision and pattern recognition*, pp. 19358–19369, 2023b.
- Jiyang Gao, Chen Sun, Zhenheng Yang, and Ram Nevatia. Tall: Temporal activity localization via language query. In *Proceedings of the IEEE international conference on computer vision*, pp. 5267–5275, 2017.

- Alex Gorban, Haroon Idrees, Yu-Gang Jiang, A. Roshan Zamir, Ivan Laptev, Mubarak Shah, and Rahul Sukthankar. Thumos challenge: Action recognition with a large number of classes, 2015.
- Kristen Grauman, Andrew Westbury, Eugene Byrne, Zachary Chavis, Antonino Furnari, Rohit Girdhar, Jackson Hamburger, Hao Jiang, Miao Liu, Xingyu Liu, et al. Ego4d: Around the world in 3,000 hours of egocentric video. In *Proceedings of the IEEE/CVF conference on computer vision and pattern recognition*, pp. 18995–19012, 2022.
- Yongxin Guo, Jingyu Liu, Mingda Li, Dingxin Cheng, Xiaoying Tang, Dianbo Sui, Qingbin Liu, Xi Chen, and Kevin Zhao. Vtg-llm: Integrating timestamp knowledge into video llms for enhanced video temporal grounding. In *Proceedings of the AAAI Conference on Artificial Intelligence*, volume 39, pp. 3302–3310, 2025a.
- Yongxin Guo, Jingyu Liu, Mingda Li, Qingbin Liu, Xi Chen, and Xiaoying Tang. TRACE: Temporal grounding video LLM via causal event modeling. In *The Thirteenth International Conference on Learning Representations*, 2025b. URL <https://openreview.net/forum?id=14fFV0chUS>.
- Michael Gygli, Helmut Grabner, Hayko Riemenschneider, and Luc Van Gool. Creating Summaries from User Videos. In David Fleet, Tomas Pajdla, Bernt Schiele, and Tinne Tuytelaars (eds.), *ECCV*, pp. 505–520, 2014. doi: 10.1007/978-3-319-10584-0_33.
- Kaiming He, Haoqi Fan, Yuxin Wu, Saining Xie, and Ross Girshick. Momentum contrast for unsupervised visual representation learning. In *Proceedings of the IEEE/CVF conference on computer vision and pattern recognition*, pp. 9729–9738, 2020.
- Edward J. Hu, Yelong Shen, Phillip Wallis, Zeyuan Allen-Zhu, Yuanzhi Li, Shean Wang, Lu Wang, and Weizhu Chen. Lora: Low-rank adaptation of large language models, 2021. URL <https://arxiv.org/abs/2106.09685>.
- Bin Huang, Xin Wang, Hong Chen, Zihan Song, and Wenwu Zhu. Vtimellm: Empower llm to grasp video moments. In *Proceedings of the IEEE/CVF Conference on Computer Vision and Pattern Recognition*, pp. 14271–14280, 2024.
- De-An Huang, Shijia Liao, Subhashree Radhakrishnan, Hongxu Yin, Pavlo Molchanov, Zhiding Yu, and Jan Kautz. Lita: Language instructed temporal-localization assistant. In *European Conference on Computer Vision*, pp. 202–218. Springer, 2025.
- Yu-Gang Jiang, Jingen Liu, A. Roshan Zamir, George Toderici, Ivan Laptev, Mubarak Shah, and Rahul Sukthankar. Thumos challenge: Action recognition with a large number of classes, 2014.
- Takeshi Kojima, Shixiang Shane Gu, Machel Reid, Yutaka Matsuo, and Yusuke Iwasawa. Large language models are zero-shot reasoners. *Advances in neural information processing systems*, 35:22199–22213, 2022.
- Ranjay Krishna, Kenji Hata, Frederic Ren, Li Fei-Fei, and Juan Carlos Niebles. Dense-captioning events in videos. In *Proceedings of the IEEE international conference on computer vision*, pp. 706–715, 2017.
- Xin Lai, Zhuotao Tian, Yukang Chen, Yanwei Li, Yuhui Yuan, Shu Liu, and Jiaya Jia. Lisa: Reasoning segmentation via large language model. In *Proceedings of the IEEE/CVF Conference on Computer Vision and Pattern Recognition (CVPR)*, pp. 9579–9589, June 2024.
- Jie Lei, Tamara L Berg, and Mohit Bansal. Detecting moments and highlights in videos via natural language queries. *Advances in Neural Information Processing Systems*, 34:11846–11858, 2021.
- Bo Li, Yuanhan Zhang, Dong Guo, et al. Llava-onevision: Easy visual task transfer. *arXiv preprint arXiv:2408.03326*, 2024.
- Junnan Li, Dongxu Li, Silvio Savarese, and Steven Hoi. Blip-2: Bootstrapping language-image pre-training with frozen image encoders and large language models. In *International conference on machine learning*, pp. 19730–19742. PMLR, 2023.

- Yanwei Li, Chengyao Wang, and Jiaya Jia. Llama-vid: An image is worth 2 tokens in large language models. In *European Conference on Computer Vision*, pp. 323–340. Springer, 2025.
- Bin Lin, Yang Ye, Bin Zhu, Jiayi Cui, Munan Ning, Peng Jin, and Li Yuan. Video-llava: Learning united visual representation by alignment before projection. *arXiv preprint arXiv:2311.10122*, 2023a.
- Kevin Lin, Faisal Ahmed, Linjie Li, Chung-Ching Lin, Ehsan Azarnasab, Zhengyuan Yang, Jianfeng Wang, Lin Liang, Zicheng Liu, Yumao Lu, et al. Mm-vid: Advancing video understanding with gpt-4v (ision). *arXiv preprint arXiv:2310.19773*, 2023b.
- Kevin Qinghong Lin, Pengchuan Zhang, Joya Chen, Shraman Pramanick, Difei Gao, Alex Jinpeng Wang, Rui Yan, and Mike Zheng Shou. Univtg: Towards unified video-language temporal grounding. In *Proceedings of the IEEE/CVF International Conference on Computer Vision (ICCV)*, pp. 2794–2804, October 2023c.
- Haotian Liu, Chunyuan Li, Qingyang Wu, and Yong Jae Lee. Visual instruction tuning. *Advances in neural information processing systems*, 36, 2024a.
- Ye Liu, Siyuan Li, Yang Wu, Chang-Wen Chen, Ying Shan, and Xiaohu Qie. Umt: Unified multi-modal transformers for joint video moment retrieval and highlight detection. In *Proceedings of the IEEE/CVF conference on computer vision and pattern recognition*, pp. 3042–3051, 2022.
- Ye Liu, Jixuan He, Wanhua Li, Junsik Kim, Donglai Wei, Hanspeter Pfister, and Chang Wen Chen. r^2 -tuning: Efficient image-to-video transfer learning for video temporal grounding, 2024b. URL <https://arxiv.org/abs/2404.00801>.
- Ye Liu, Zongyang Ma, Zhongang Qi, Yang Wu, Ying Shan, and Chang W Chen. Et bench: Towards open-ended event-level video-language understanding. *Advances in Neural Information Processing Systems*, 37:32076–32110, 2024c.
- Weiheng Lu, Jian Li, An Yu, Ming-Ching Chang, Shengpeng Ji, and Min Xia. Llava-mr: Large language-and-vision assistant for video moment retrieval. *arXiv preprint arXiv:2411.14505*, 2024.
- Muhammad Maaz, Hanoona Rasheed, Salman Khan, and Fahad Shahbaz Khan. Video-chatgpt: Towards detailed video understanding via large vision and language models. *arXiv preprint arXiv:2306.05424*, 2023.
- Boris Meinardus, Hector Rodriguez, Anil Batra, Anna Rohrbach, and Marcus Rohrbach. Chrono: A simple blueprint for representing time in mllms. *arXiv preprint arXiv:2406.18113*, 2024.
- WonJun Moon, Sangeek Hyun, SuBeen Lee, and Jae-Pil Heo. Correlation-guided query-dependency calibration for video temporal grounding. *arXiv preprint arXiv:2311.08835*, 2023a.
- WonJun Moon, Sangeek Hyun, SangUk Park, Dongchan Park, and Jae-Pil Heo. Query-dependent video representation for moment retrieval and highlight detection. In *Proceedings of the IEEE/CVF conference on computer vision and pattern recognition*, pp. 23023–23033, 2023b.
- OpenAI. Gpt-4o system card, 2024. URL <https://arxiv.org/abs/2410.21276>.
- Maxime Oquab, Timothée Darcet, Théo Moutakanni, Huy Vo, Marc Szafraniec, Vasil Khalidov, Pierre Fernandez, Daniel Haziza, Francisco Massa, Alaaeldin El-Nouby, et al. Dinov2: Learning robust visual features without supervision. *arXiv preprint arXiv:2304.07193*, 2023.
- Mayu Otani, Yuta Nakashima, Esa Rahtu, and Janne Heikkilä. Uncovering hidden challenges in query-based video moment retrieval. *arXiv preprint arXiv:2009.00325*, 2020.
- Long Ouyang, Jeffrey Wu, Xu Jiang, Diogo Almeida, Carroll Wainwright, Pamela Mishkin, Chong Zhang, Sandhini Agarwal, Katarina Slama, Alex Ray, et al. Training language models to follow instructions with human feedback. *Advances in neural information processing systems*, 35: 27730–27744, 2022.

- Zongshang Pang, Yuta Nakashima, Mayu Otani, and Hajime Nagahara. Contrastive Losses Are Natural Criteria for Unsupervised Video Summarization. In *Proceedings of the IEEE/CVF Winter Conference on Applications of Computer Vision*, pp. 2010–2019, 2023.
- Zongshang Pang, Yuta Nakashima, Mayu Otani, and Hajime Nagahara. Revisiting pixel-level contrastive pre-training on scene images. In *Proceedings of the IEEE/CVF winter conference on applications of computer vision*, pp. 1784–1793, 2024.
- Viorica Patraucean, Lucas Smaira, Ankush Gupta, Adria Recasens, Larisa Markeeva, Dylan Bannarse, Skanda Koppula, Mateusz Malinowski, Yi Yang, Carl Doersch, et al. Perception test: A diagnostic benchmark for multimodal video models. *Advances in Neural Information Processing Systems*, 36:42748–42761, 2023.
- Long Qian, Juncheng Li, Yu Wu, Yaobo Ye, Hao Fei, Tat-Seng Chua, Yueting Zhuang, and Siliang Tang. Momentor: Advancing video large language model with fine-grained temporal reasoning. *arXiv preprint arXiv:2402.11435*, 2024.
- Rui Qian, Shuangrui Ding, Xiaoyi Dong, Pan Zhang, Yuhang Zang, Yuhang Cao, Dahua Lin, and Jiaqi Wang. Dispider: Enabling video llms with active real-time interaction via disentangled perception, decision, and reaction. In *Proceedings of the Computer Vision and Pattern Recognition Conference*, pp. 24045–24055, 2025.
- Alec Radford, Jong Wook Kim, Chris Hallacy, Aditya Ramesh, Gabriel Goh, Sandhini Agarwal, Girish Sastry, Amanda Askell, Pamela Mishkin, Jack Clark, et al. Learning transferable visual models from natural language supervision. In *International conference on machine learning*, pp. 8748–8763. PMLR, 2021.
- Shuhuai Ren, Linli Yao, Shicheng Li, Xu Sun, and Lu Hou. Timechat: A time-sensitive multimodal large language model for long video understanding. In *Proceedings of the IEEE/CVF Conference on Computer Vision and Pattern Recognition*, pp. 14313–14323, 2024.
- Enxin Song, Wenhao Chai, Guanhong Wang, Yucheng Zhang, Haoyang Zhou, Feiyang Wu, Haozhe Chi, Xun Guo, Tian Ye, Yanting Zhang, et al. Moviechat: From dense token to sparse memory for long video understanding. In *Proceedings of the IEEE/CVF Conference on Computer Vision and Pattern Recognition*, pp. 18221–18232, 2024.
- Yale Song, Jordi Vallmitjana, Amanda Stent, and Alejandro Jaimes. Tvsum: Summarizing web videos using titles. In *Proceedings of the IEEE conference on computer vision and pattern recognition*, pp. 5179–5187, 2015.
- Dídac Surís, Sachit Menon, and Carl Vondrick. Vipergpt: Visual inference via python execution for reasoning. In *Proceedings of the IEEE/CVF International Conference on Computer Vision*, pp. 11888–11898, 2023.
- Jiawei Wang, Liping Yuan, Yuchen Zhang, and Haomiao Sun. Tarsier: Recipes for training and evaluating large video description models. *arXiv preprint arXiv:2407.00634*, 2024a.
- Peng Wang, Shuai Bai, Sinan Tan, Shijie Wang, Zhihao Fan, Jinze Bai, Keqin Chen, Xuejing Liu, Jialin Wang, Wenbin Ge, et al. Qwen2-vl: Enhancing vision-language model’s perception of the world at any resolution. *arXiv preprint arXiv:2409.12191*, 2024b.
- Teng Wang, Ruimao Zhang, Zhichao Lu, Feng Zheng, Ran Cheng, and Ping Luo. End-to-end dense video captioning with parallel decoding. In *Proceedings of the IEEE/CVF international conference on computer vision*, pp. 6847–6857, 2021a.
- Xidong Wang, Dingjie Song, Shunian Chen, Chen Zhang, and Benyou Wang. Longllava: Scaling multi-modal llms to 1000 images efficiently via hybrid architecture. *arXiv preprint arXiv:2409.02889*, 2024c.
- Xinlong Wang, Rufeng Zhang, Chunhua Shen, Tao Kong, and Lei Li. Dense contrastive learning for self-supervised visual pre-training. In *Proceedings of the IEEE/CVF conference on computer vision and pattern recognition*, pp. 3024–3033, 2021b.

- Yueqian Wang, Xiaojun Meng, Jianxin Liang, Yuxuan Wang, Qun Liu, and Dongyan Zhao. Hawk-eye: Training video-text llms for grounding text in videos. *arXiv preprint arXiv:2403.10228*, 2024d.
- Jason Wei, Xuezhi Wang, Dale Schuurmans, Maarten Bosma, Fei Xia, Ed Chi, Quoc V Le, Denny Zhou, et al. Chain-of-thought prompting elicits reasoning in large language models. *Advances in neural information processing systems*, 35:24824–24837, 2022.
- Yongliang Wu, Xinting Hu, Yuyang Sun, Yizhou Zhou, Wenbo Zhu, Fengyun Rao, Bernt Schiele, and Xu Yang. Number it: Temporal grounding videos like flipping manga. In *Proceedings of the Computer Vision and Pattern Recognition Conference*, pp. 13754–13765, 2025.
- Lin Xu, Yilin Zhao, Daquan Zhou, Zhijie Lin, See Kiong Ng, and Jiashi Feng. Pllava : Parameter-free llava extension from images to videos for video dense captioning, 2024. URL <https://arxiv.org/abs/2404.16994>.
- Fuzhao Xue, Yukang Chen, Dacheng Li, Qinghao Hu, Ligeng Zhu, Xiuyu Li, Yunhao Fang, Haotian Tang, Shang Yang, Zhijian Liu, et al. Longvila: Scaling long-context visual language models for long videos. *arXiv preprint arXiv:2408.10188*, 2024.
- Shen Yan, Xuehan Xiong, Arsha Nagrani, Anurag Arnab, Zhonghao Wang, Weina Ge, David Ross, and Cordelia Schmid. Unloc: A unified framework for video localization tasks. In *Proceedings of the IEEE/CVF International Conference on Computer Vision (ICCV)*, pp. 13623–13633, October 2023.
- Antoine Yang, Arsha Nagrani, Paul Hongsuck Seo, Antoine Miech, Jordi Pont-Tuset, Ivan Laptev, Josef Sivic, and Cordelia Schmid. Vid2seq: Large-scale pretraining of a visual language model for dense video captioning. In *Proceedings of the IEEE/CVF Conference on Computer Vision and Pattern Recognition*, pp. 10714–10726, 2023.
- Yuan Yao, Tianyu Yu, Ao Zhang, et al. Minicpm-v: A gpt-4v level mllm on your phone, 2024. URL <https://arxiv.org/abs/2408.01800>.
- Liping Yuan, Jiawei Wang, Haomiao Sun, Yuchen Zhang, and Yuan Lin. Tarsier2: Advancing large vision-language models from detailed video description to comprehensive video understanding. *arXiv preprint arXiv:2501.07888*, 2025.
- Abhay Zala, Jaemin Cho, Satwik Kottur, Xilun Chen, Barlas Oguz, Yashar Mehdad, and Mohit Bansal. Hierarchical video-moment retrieval and step-captioning. In *Proceedings of the IEEE/CVF Conference on Computer Vision and Pattern Recognition*, pp. 23056–23065, 2023.
- Andy Zeng, Maria Attarian, Brian Ichter, Krzysztof Choromanski, Adrian Wong, Stefan Welker, Federico Tombari, Aveek Purohit, Michael Ryoo, Vikas Sindhwani, et al. Socratic models: Composing zero-shot multimodal reasoning with language. *arXiv preprint arXiv:2204.00598*, 2022.
- Xiangyu Zeng, Kunchang Li, Chenting Wang, Xinhao Li, Tianxiang Jiang, Ziang Yan, Songze Li, Yansong Shi, Zhengrong Yue, Yi Wang, Yali Wang, Yu Qiao, and Limin Wang. Timesuite: Improving MLLMs for long video understanding via grounded tuning. In *The Thirteenth International Conference on Learning Representations*, 2025. URL <https://openreview.net/forum?id=nAVejJURqZ>.
- Xiaohua Zhai, Basil Mustafa, Alexander Kolesnikov, and Lucas Beyer. Sigmoid loss for language image pre-training. In *Proceedings of the IEEE/CVF international conference on computer vision*, pp. 11975–11986, 2023.
- Hang Zhang, Xin Li, and Lidong Bing. Video-llama: An instruction-tuned audio-visual language model for video understanding. *arXiv preprint arXiv:2306.02858*, 2023.
- Peiyuan Zhang, Kaichen Zhang, Bo Li, Guangtao Zeng, Jingkang Yang, Yuanhan Zhang, Ziyue Wang, Haoran Tan, Chunyuan Li, and Ziwei Liu. Long context transfer from language to vision. *arXiv preprint arXiv:2406.16852*, 2024.
- Luowei Zhou, Chenliang Xu, and Jason Corso. Towards automatic learning of procedures from web instructional videos. In *Proceedings of the AAAI conference on artificial intelligence*, 2018.

Dimitri Zhukov, Jean-Baptiste Alayrac, Ramazan Gokberk Cinbis, David Fouhey, Ivan Laptev, and Josef Sivic. Cross-task weakly supervised learning from instructional videos. In *Proceedings of the IEEE/CVF Conference on Computer Vision and Pattern Recognition*, pp. 3537–3545, 2019.

A THE USE OF LARGE LANGUAGE MODELS (LLMs)

During the drafting and revision of this manuscript, we used GPT5 and Claude Opus 4.1 for checking grammatical errors, formatting the LaTeX code for tables and figures, and getting suggestions on academic writing.

B IMPLEMENTATION DETAILS

Following E.T.Chat, we perform three stages of training. Throughout all three stages, the visual encoder remains frozen while the frame compressor and projection layer are trainable. In stage 1, we additionally freeze the Q-Former and LLM. In stage 2, we unfreeze the Q-Former and train the LLM with LoRA. In stage 3, we conduct fine-tuning by freezing part of the Q-Former, initializing a new LoRA module for the LLM, and initializing two MLP projectors for the frame and structural token hidden states, respectively, for the structural token grounding module. Following (Liu et al., 2024c), the structural token hidden states are extracted from the second-to-last LLM layer and the frame hidden states from the last layer. Table 8 provides the detailed hyperparameter setup used for stage-3 training. All training was performed on 4 NVIDIA A100-80G GPUs.

We develop MeCo using the E.T.Chat architecture (Liu et al., 2024c), which employs a pre-trained ViT-G/14 from EVA-CLIP (Fang et al., 2023b) as the visual encoder and a resampler consisting of a pre-trained instruction-conditioned Q-Former (Li et al., 2023) followed by a frame compressor (Liu et al., 2024c) that produces one token per video frame. A projection layer projects visual tokens into LLM inputs. The QWen2 base LLM (Wang et al., 2024b) is from MiniCPM-V-2.6 (Yao et al., 2024). We also implemented MeCo with QWen2VL-7B Wang et al. (2024b) by mounting two newly initialized projects from ETChat. For pre-training, we format the structural token sequence based on the temporal order of event and transition segments. For dataset-wise fine-tuning, we observed that the temporal order of structural tokens may inherit the dataset-specific biases in the temporal positions of ground-truth windows (Otani et al., 2020). Therefore, we relax the format of the structural token sequence by simply appending a single `< t s t >` token to the end which attends to all the transition frames during training and inference.

Table 8: Hyperparameters for stage-3 training.

| MLP Projectors | |
|--------------------------|------------|
| Number of Layers | 2 |
| Hidden Size | 1536 |
| Output Size | 3072 |
| Large Range LoRA | |
| LoRA r | 128 |
| LoRA α | 256 |
| LoRA Dropout | 0.05 |
| LoRA Modules | QVO Layers |
| Model Training | |
| Max Number of Tokens | 2048 |
| Number of Epochs | 1 |
| Batch Size | 2 |
| Learning Rate for LoRA | 5e-5 |
| LR Decay Type | Cosine |
| Warmup Ratio | 0.03 |
| Optimizer | AdamW |
| AdamW β_1, β_2 | 0.9, 0.997 |

C QUERY-FOCUSED CAPTIONING

Based on the temporal localization data in E.T.Instruct (Liu et al., 2024c), we extract event segments and input them to a video captioning model, MiniCPM-V-2.6 (Yao et al., 2024), to generate detailed captions. As these captions often contain redundant information, we summarize them using GPT-4o-mini (OpenAI, 2024) under the condition that the final captions are more detailed than the original localization queries. The annotation pipeline and representative QFC examples are shown in Fig. 5

D ADAPTING TIMECHAT AND VTGLLM TO WORK WITH MECO

In Tab. 4, we show the results of integrating MeCo into the TimeChat (Ren et al., 2024) and VTGLLM (Guo et al., 2025b) models. TimeChat and VTGLLM share the same architecture, with a ViT-G/14 from EVA-CLIP (Fang et al., 2023b) as the visual encoder, a pre-trained Q-Former (Li et al., 2023) as the visual resampler, and VideoLLaMa (Zhang et al., 2023) as the base video LLM. The key difference is that TimeChat applies a sliding video Q-Former to compress the visual tokens to 96, while VTGLLM applies a slot-based visual compressor to obtain 256 tokens. Both use 96 as the maximum number of sampled frames.

To integrate MeCo into this architecture, we modify the video Q-Former in TimeChat to a standard image Q-Former, which resamples 32 tokens to 1 token per frame. Additionally, we apply bidirectional self-attention to the visual token components, following (Liu et al., 2024c). Other components remain unchanged. We then train TimeChat, VTGLLM, and MeCo (adapted) on E.T.Instruct using the same hyperparameters as in (Ren et al., 2024).

E MECO INFERENCE

We provide the pseudo code for MeCo’s inference process in Algorithm 1. Specifically, after the LLM finishes its generation, we first extract all the structural tokens from the LLM’s generated token indices and extract the indices of the event tokens (`<ent>`) `ent_idxes` in the extracted structural token list. We then obtain the frame embeddings `fr_emb` and the structural token embeddings `st_emb` by extracting the LLM hidden states and feeding them into the MLP projectors. The pair-wise cosine similarities between the two sets of embeddings are then calculated, which can then be normalized by a `softmax()` operation along the temporal axis to obtain the conditional probability `p_hs` in Eq. (5). Each frame is then assigned to the structural token that leads to be highest conditional probability using the `argmax()` operation. For each `<ent>` token, we find all the frames that have been assigned to it, merge temporally consecutive frames into segments by `split_at_gaps`, and add the obtained segments into `ent_segs` (we observed that sometimes the LLM tends to represent multiple semantically-relevant segments by a single `<ent>`). The start and end timestamps for each segment are simply the `timesatmps` of the first and last frames in the segment. We do not conduct post-processing for cases where the segment timestamps do not follow the appearance order of their corresponding `<ent>` tokens. The above pseudo code assumes the most common case where all the event segments are non-overlapping for a clean demonstration of the inference process. In the actual implementation, we process each `<ent>` token one by one and assign frames to each `<ent>` token after suppressing its adjacent `<ent>` tokens’ (if any) frame scores to take care of overlapping cases.

F FAILURE CASES

In Fig. 6, we visualize several typical failure cases: (a) the `<ent>` token attends to the totally wrong segment; (b) the `<ent>` token attends to the correct semantic information but the boundaries are not well estimated by the `<tst>` tokens; (c) the model only generates one events while there are actually three; (d) the video starts directly with the event segment while the model considers the first few frames as transition frames and thus generates a `<tst>` token at first.

Algorithm 1 Pseudocode of MeCo Inference.

```

# fr_emb: frame embeddings (TxC)
# st_emb: structural token embeddings ((M+K)xC)
# tau: temperature
# ent_idces: indices of event tokens <ent>

# Calculate conditional probabilities (Eq. (5))
zfr = l2_normalize(fr_emb)
zst = l2_normalize(st_emb)
sim = matmul(zfr, zst.T) # Tx(M+K)
p_hs = softmax(sim / tau, dim=0) # Eq. (5)

# Assign frames to structural tokens
assign = p_hs.argmax(dim=1)

ent_segs = []
for i, idx in enumerate(ent_idces):
    # Get indices where assign == idx
    indices = where(assign == idx)

    # Split at discontinuities to get segments
    segs = split_at_gaps(indices)

    # Get start and end timestamps
    timestamps = [[seg[0], seg[1]] for seg in segs]

    # Add to the segment list
    ent_segs.extend(segs) # [[ts_1, te_1], [ts_2, te_2], ...]

```

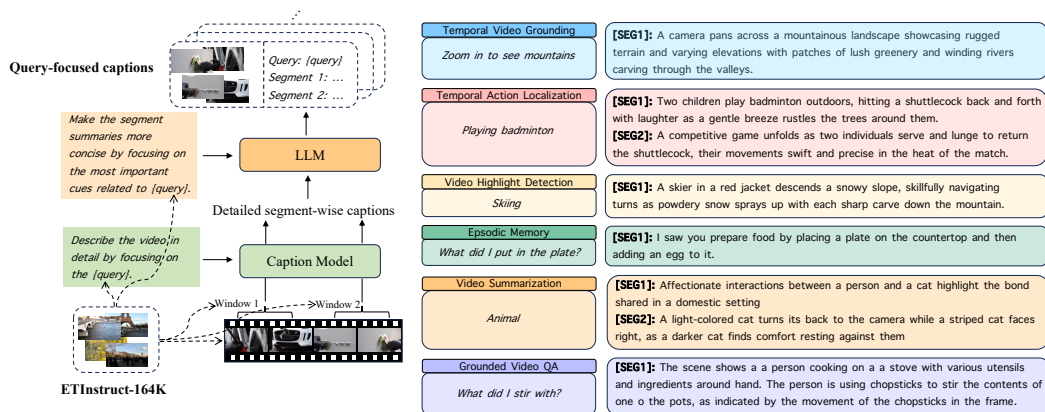


Figure 5: Query-focused captioning pipeline and examples.

G EVALUATION AND TRAINING PROMPT TEMPLATES

For evaluation, we modify E.T.Bench templates to work with MeCo. Example templates are provided in Figure 7. For training, we manually craft a query-focused captioning-aware instruction template for each task domain in E.T.Instruct and diversify it with GPT-4o (OpenAI, 2024) to generate four additional templates. The instruction templates for all domains are provided in Fig. 8.

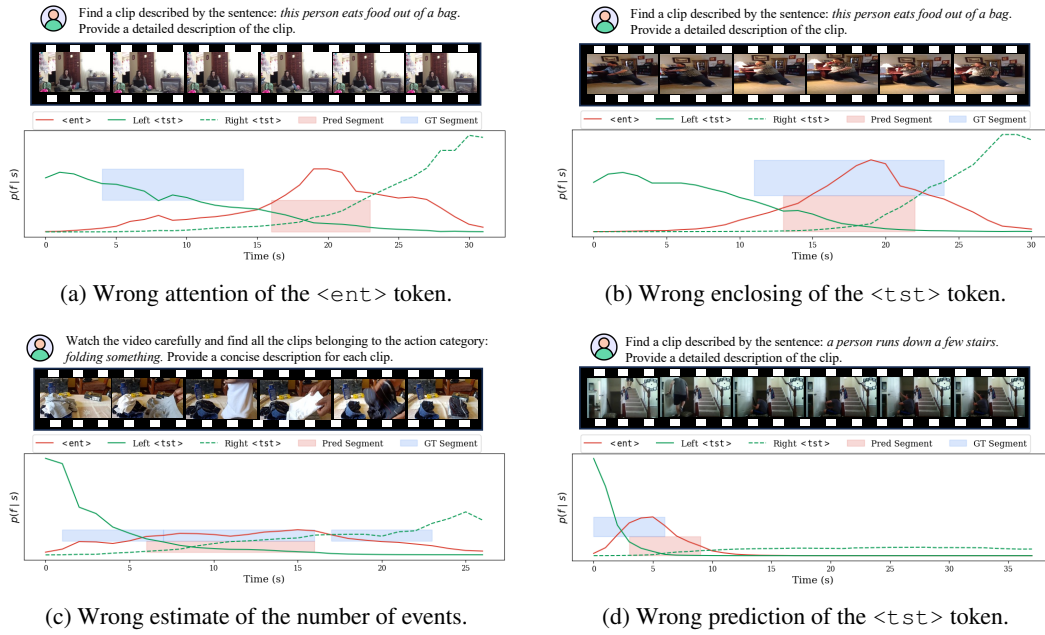


Figure 6: Visualization of figure cases.

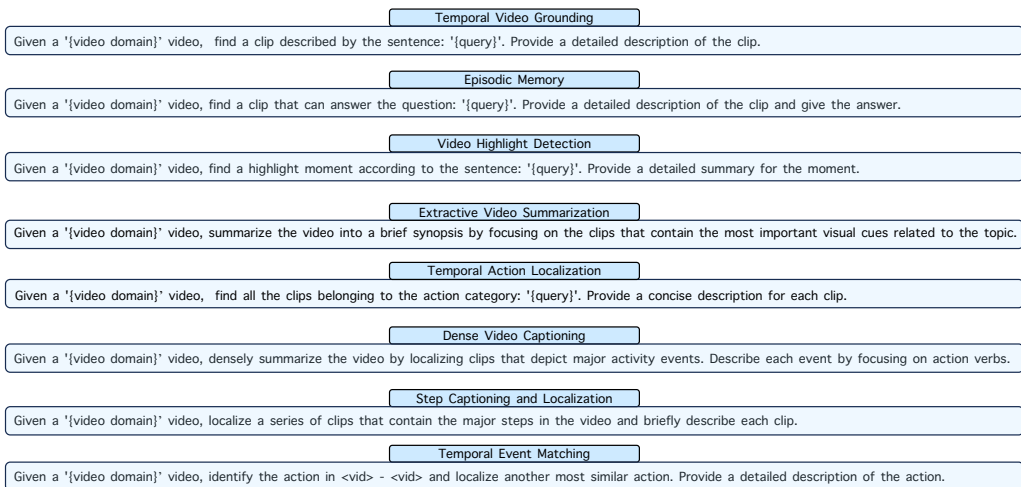
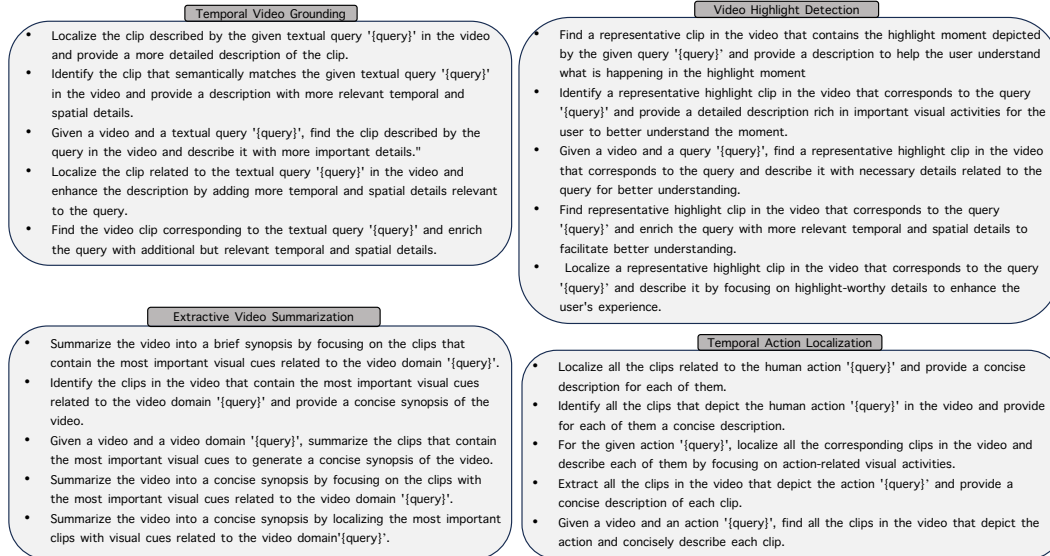
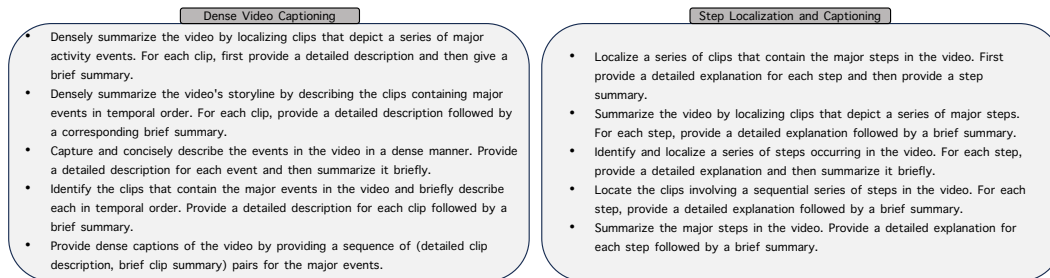


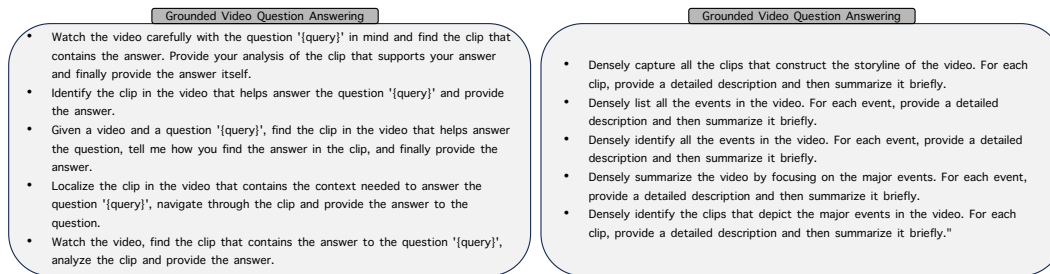
Figure 7: Evaluation prompt templates.



(a) Temporal grounding.



(b) Dense video captioning.



(c) Complex reasoning.

Figure 8: Instruction templates for different task domains: (a) temporal grounding, (b) dense video captioning, and (c) complex reasoning.